HOSTED BY

ELSEVIER

Available online at www.sciencedirect.com

ScienceDirect

Grain yield losses in yellow-rusted durum wheat estimated using digital and conventional parameters under field conditions

Omar Vergara-Diaz[a], *Shawn C. Kefauver*[a,*], *Abdelhalim Elazab*[a], *Maria Teresa Nieto-Taladriz*[b], *José Luis Araus*[a]

[a]*Unit of Plant Physiology, Department of Plant Biology, Faculty of Biology, University of Barcelona, Diagonal 645, 08028 Barcelona, Spain*
[b]*National Institute for Agricultural and Food Research and Technology (INIA), Ctra de la Coruña 7.5, 28040, Madrid Spain*

ARTICLE INFO

Article history:
Received 17 December 2014
Received in revised form
25 February 2015
Accepted 3 March 2015
Available online 11 April 2015

Keywords:
Wheat yellow rust
Field phenotyping
NDVI
Phenology, *Puccinia striiformis*
RGB-based indices
Triticum durum

ABSTRACT

The biotrophic fungus *Puccinia striiformis* f. sp. *tritici* is the causal agent of the yellow rust in wheat. Between the years 2010–2013 a new strain of this pathogen (Warrior/Ambition), against which the present cultivated wheat varieties have no resistance, appeared and spread rapidly. It threatens cereal production in most of Europe. The search for sources of resistance to this strain is proposed as the most efficient and safe solution to ensure high grain production. This will be helped by the development of high performance and low cost techniques for field phenotyping. In this study we analyzed vegetation indices in the Red, Green, Blue (RGB) images of crop canopies under field conditions. We evaluated their accuracy in predicting grain yield and assessing disease severity in comparison to other field measurements including the Normalized Difference Vegetation Index (NDVI), leaf chlorophyll content, stomatal conductance, and canopy temperature. We also discuss yield components and agronomic parameters in relation to grain yield and disease severity. RGB-based indices proved to be accurate predictors of grain yield and grain yield losses associated with yellow rust (R^2 = 0.581 and R^2 = 0.536, respectively), far surpassing the predictive ability of NDVI (R^2 = 0.118 and R^2 = 0.128, respectively). In comparison to potential yield, we found the presence of disease to be correlated with reductions in the number of grains per spike, grains per square meter, kernel weight and harvest index. Grain yield losses in the presence of yellow rust were also greater in later heading varieties. The combination of RGB-based indices and days to heading together explained 70.9% of the variability in grain yield and 62.7% of the yield losses.

* *Corresponding author.*
E-mail address: sckefauver@ub.edu (S.C. Kefauver).
Peer review under responsibility of Crop Science Society of China and Institute of Crop Science, CAAS.

http://dx.doi.org/10.1016/j.cj.2015.03.003

1. Introduction

Wheat is the second most cultivated cereal in Spain [1] and the most widely cultivated cereal worldwide, with over 218 Mha in cultivation [2]. *Puccinia striiformis* is the causal agent of yellow rust in grasses and has been described as infecting a wide variety of cultivated cereals, including wheat, rye, barley and triticale. The *forma specialis* (f. sp.) *tritici* primarily infects wheat. The presence and severity of this fungal disease in Mediterranean and temperate cultivars has not been of importance until recently. The use of wheat varieties resistant to this pathogen had previously ensured that losses were minimal in the Mediterranean region [3]; however, the presence of a new *Pst* race called the Warrior/Ambition race, first described during 2009/2010 in the United Kingdom, Germany, Denmark, France and Scandinavia, has severely affected winter wheat production in recent years [4]. One year after it was first discovered in Europe, its presence was also detected in Spain [4] and the disease spread extensively during the 2012/2013 winter wheat season. Several epidemic events resulting in serious crop damage and widespread yield losses in Spain [3] have since been recorded. The rapid spread of this strain was favored by the climatic conditions of the 2012/2013 season: cool temperatures during spring, high humidity and prolonged rainy conditions [5].

P. striiformis f. sp. *tritici* has a great capacity for dispersal and for variation [6]. The new Warrior/Ambition strain is virulent for most of the currently deployed resistance genes [3] and can therefore parasitize most of the wheat varieties presently grown around the world. In addition, this fungus spreads by wind over hundreds of kilometers, germinates quickly at low temperatures (7–10 °C) [6,7], and infects wheat crops at a relatively early growth stage. The most apparent visible sign of infection is the orange-yellowish mass of urediniospores being produced by uredinia arranged in long, narrow stripes along the leaf veins. Development of resistant varieties is essential for effective control; however, to date no variety with resistance to the strain has been recommended in Spain [8]. There is an urgent need to develop improved high throughput field phenotyping approaches for breeding for yellow rust resistance in wheat.

The diversity of existing wheat varieties provides a source of genetic variability from which we can select a high number of features of interest, such as drought and salinity tolerance, improvements in nutrient use efficiency or, in our case, disease resistance. Phenomics arises as a complex and integrative discipline that tries to characterize plant functional traits related to specific conditions from the cell to community level. However, it is considered a major bottleneck with regard to the advancement of crop breeding [9–13]. Thus, high-performance phenotyping systems are required to understand the relationships between genotype, phenotype and environment. Phenotyping requires that the studied trait and the chosen methodology for its measurement are appropriate for the purpose of the investigation.

There are currently several criteria for field phenotyping by monitoring and analyzing different plant traits as a response to stress conditions. However, most of these techniques are time-consuming, unrepresentative of the whole plot and/or require sampling, laboratory processing and costly equipment. Visible and near infrared (VNIR) spectral measurements have high performance in characterizing physiological and biochemical processes as well as agronomic traits at both crop and leaf levels [14–20], whereas, thermal imaging enables rapid observations of plant water status and their cooling ability [9,10]. Both approaches can be integrated as part of field-monitoring platforms, but their implementation is expensive. As an alternative, vegetation indices based on conventional digital Red, Green, Blue (RGB) digital imaging are high-performance, low-cost techniques for predicting plant and crop traits, and can be based on processing pictures of either crop canopies or single leaves [21]. The use of these technologies is currently expanding due to their versatility and affordability. Some of their proven applications are: the development of predictive models for crop yield under specific growing conditions [22], crop growth assessment under water stress conditions [23], fertilization monitoring and nitrogen requirements [24], LAI (leaf area index) for lodging risk evaluation in winter wheat [25], and quantification of pollen release [26].

The efficacy of RGB digital methods for the evaluation of a pest or disease at the leaf level has also been reported, including powdery mildew on cucumber leaves [27], assessment of foliar disease symptom severities in corn, wheat and soybean [28], determination of the impact of disease severity of specific grain diseases [29], and of different types of fungal diseases in wheat [30,31]. In all these cases image analysis techniques were employed to detect the presence of the pest or disease and the infected, necrotic and/or dry areas using scans or photographic images of leaves or other plant parts. This approach has proven highly accurate in its predictions, but is cumbersome and time consuming in practice because it requires manually intensive and destructive harvesting and photographing the plant organs of interest. Studies on sensitivity of crops to biotic stress using hyperspectral crop canopy data have been conducted previously [32–35], but no previous studies using digital RGB cameras at the canopy level are known to the authors. Thus, the development of prediction models of grain yield (GY) and crop pathogen sensitivity using digital RGB photography of crop canopies represents a novel and practical alternative to other remote sensing approaches, such as VNIR-derived vegetation indices, for wheat phenotyping under field conditions.

The objective of this study was to assess the sensitivity of autumn sown wheat varieties to yellow rust under field conditions using different methodologies. First, we assessed the performance and accuracy of RGB indices in comparison to the Normalized Difference Vegetation Index (NDVI) for prediction of grain yield losses associated with yellow rust. Second, we evaluated the performance of other agronomic metrics commonly used in field phenotyping (leaf chlorophyll content, stomatal conductance and canopy temperature) and their relationships with GY and disease severity. Third, we investigated the effects of yellow rust on the relationships between common agronomic parameters, GY and the grain yield loss index (GYLI). Finally, we combined the best remotely-sensed vegetation indices and agronomic metrics in stepwise multivariate predictive models of GY and GYLI.

2. Materials and methods

2.1. Experimental field, plant material and growing conditions

Field trials were carried out at the experimental station of Colmenar de Oreja (40° 04′ N, 3° 31′ W) belonging to the Instituto Nacional de Investigación y Tecnología Agraria y Alimentaria (INIA) of Spain during the 2012/2013 crop season. The average annual precipitation corresponding to this region is about 425 mm and the average annual temperature is 13.7 °C. The region has an altitude of 590 m in the middle of the Tajo River basin. The ground has a slightly alkaline soil (pH 8.1) and corresponds to a xerofluvent soil [36]. It is a kind of alluvial entisol with a xeric moisture regime [37]. Before planting, the field was fertilized with 400 kg ha^{-1} of a 15:15:15 N:P:K (15% N, 15% P_2O_5, 15% K_2O) fertilizer. A second application of 150 kg ha^{-1} of urea 46% dilution was applied before stem elongation.

Sixteen durum wheat varieties (*Triticum turgidum* L. subsp. *durum* (Desf) Husn.) were grown, 13 of Spanish registration (Vitrón, Regallo, Gallareta, Bolo, Don Pedro, Sula, Bólido, Dorondón, Murgos, Pelayo, Don Sebastian, Don Ricardo and Kiko Nick) and three European (Simeto, Claudio and Iride from Italy). The experimental design was established in randomized blocks with three replicates and a total of 48 plots. The planting took place on December 5, 2012, with a planting density of 250 seeds per square meter. The plots had an area of 7 × 1.5 m^2 and a distance of 0.2 m between rows. Rainfall during the 2012/2013 crop season was 278 mm and the average temperature was 11.4 °C. This amount of precipitation was considerably higher than the same period in previous years (200–230 mm). Furthermore, rainfall was focused in the spring months: March (106 mm), April (44 mm) and May (53 mm). The average humidity during the period was 10–15% higher than normal according to historical records [38]. This trial was not irrigated.

Field measurements and plot canopy pictures were taken five times throughout the trial: February 27–28, April 8–10, April 29–30, May 22–23 and May 30–31, 2013, corresponding with the development stages of tillering, stem elongation or jointing, heading, anthesis and post-anthesis (first half of grain filling), respectively. Plant height (PH) was measured during the last field visit. Field operators measured the number of days to heading (DH) (when approximately 50% of stems have showed half-emerged spikes). Harvesting was carried out on July 10, 2013, and grains were dried in an oven at 60 °C for 48 h. The measured traits included GY, spikes per square meter, grains per spike, thousand kernel weight (TKW) and harvest index (HI).

2.2. Disease identification of fungus

Disease was identified by station staff as yellow rust. Detailed photographs show its presence (Fig. 1) and characteristic symptoms. A camera (Pixera 150ES, USA) coupled to a zoom microscope (Olympus SZ 60, USA) was used to observe and photograph a selection of flag leaf samples from post-anthesis stage samples. These pictures show the characteristically linear lesions on the wheat leaf surface (Fig. 2). The correct identification of yellow rust was confirmed by the numerous outbreaks reported all around Spain during the same period by the Group for the Evaluation of New Varieties of Extensive Crops in Spain (GENVCE) [39] state network.

2.3. Assessment of yield losses attributed to yellow rust

As previously described, environmental conditions especially favored the development of yellow rust 2012/2013. Furthermore, continuous rains made it impossible to apply fungicides to contain the disease. Damage was evident in late April (heading stage) and worsened during the following months. In order to evaluate grain yield losses associated with the disease, grain yields of the same genotypes were measured in the following season (2013/2014) and potential yield was used as a reference. Materials in the second season were planted in the same experimental station and using a similar design and agricultural practices; the presence of rust was negligible. The average temperature during the 2013/2014 growing season

Fig. 1 – Wheat leaves damaged by yellow rust during 2012–2013.

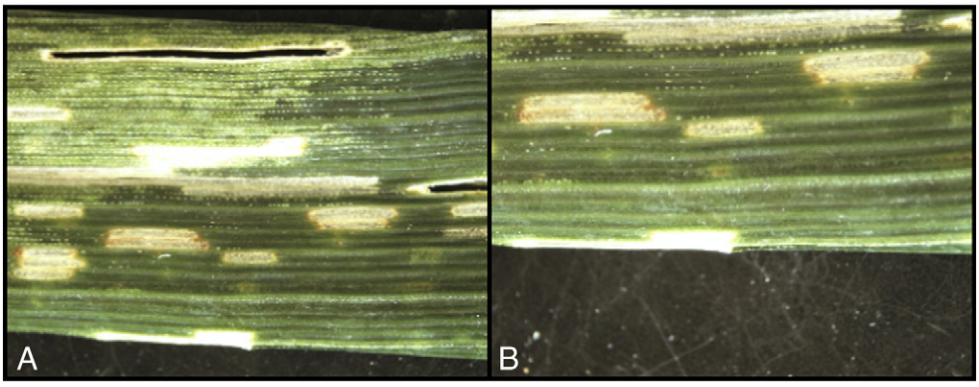

Fig. 2 – Zoomed photographs of damaged leaves.

was 13.6 °C, rainfall was 213 mm and concentrated in the cooler months: December (32 mm), January (51 mm), February (47 mm) and March (29 mm). Irrigation was also used to achieve optimal growth. Sprinkler irrigation was applied seven times, providing 355 mm of irrigation water and thus a total of 568 mm for the season. GYLI was calculated as: GYLY = (GY 2013/2014 – GY 2012/2013) / (GY 2013/2014) × 100, where GY 2013/2014 represents the potential grain yield obtained in the 2013/14 season when the yellow rust was not present, and GY 2012/2013 corresponds to grain yield in the presence of yellow rust. Finally, in order to confirm the causal relationship between the presence of the disease and the grain yield losses — ignoring possible water stress effects — grain yields from the 2013/2014 growing season (not affected by wheat rust) in rainfed conditions only, hereafter considered as sub-optimal yield conditions, were compared to grain yields of the 2012/2013 season (affected by rust).

2.4. Vegetation indices

NDVI was determined with a portable spectroradiometer (GreenSeeker handheld crop sensor, Trimble, USA) on three dates: February 27, April 10 and May 22, 2013, coincident with the development stages of tillering, jointing and anthesis, respectively. NDVI was calculated using the equation: NDVI = (NIR – R) / (NIR + R), where R is the reflectance in the red band (660 nm) and NIR is the reflectance in the near-infrared band (760 nm). The distance between the sensor and the plot canopy was 0.5–0.6 m above and perpendicular to the canopy.

One digital RGB picture was taken per plot, holding the camera at 0.8–1.0 m above the plant canopy, in a zenithal plane and focusing near the center of each plot. Photographs were taken with a Nikon D40 camera on four dates: February 27, April 8, May 23 and May 30, 2013, coincident with tillering, jointing, anthesis and post-anthesis, respectively. The D40 had a focal length of 18 mm, shutter speed of 1/125 and horizontal and vertical fields of view (FOV) of 66° 43′ and 46° 51′, respectively. No flash was used and the aperture of remained in automatic. Photographs were saved in JPEG format with a size of 1920 × 1280 pixels.

Pictures were subsequently analyzed with open source Breedpix 0.2 software designed for digital photograph processing [21]. This software enabled determination of RGB vegetation indices from the different properties of color. RGB indices were previously proven to be good indicators of plant growth and crop senescence [23]. The following five digital indices were used in this study: a*, u*, hue, green area (GA) and greener area (GAA). The last two indices analyze the number of green pixels in the image, but differ in that GAA excludes yellowish-green tones and therefore more accurately describes the amount of photosynthetically active biomass and leaf senescence. The a* and u* indices require the use of Java Advanced Imaging for calculation, and the use of formulae described by O'Gorman et al. [40] and Vrhel et al. [41], respectively, in order to analyze specific features and color components.

2.5. Leaf chlorophyll content, canopy temperature and leaf stomatal conductance

A handheld Minolta SPAD-502 sensor (Spectrum Technologies Inc., Plainfield, IL, USA) was used to measure relative leaf chlorophyll content (LCC). Five flag leaves per plot were measured at each sampling date: April 10, April 30, and May 30, 2013, corresponding to jointing, heading and post-anthesis stages, respectively. A portable thermal infra-red MIDAS 320L camera (DIAS Infrared Systems, Germany) was used to measure canopy temperatures. Photographs of whole plot were taken at midday from a distance of approximately one meter in direct sunlight. These pictures were processed using PYROSOFT Professional (DIAS Infrared Systems, Germany) for DIAS infrared cameras selecting a representative area of each plot from two dates, May 22 and May 30, 2013, corresponding to the anthesis and post-anthesis stages. Air temperature and humidity were simultaneously recorded with a thermo-hygrometer (Testo 177-H1 Logger, Germany) at the same time as each thermal picture. Air temperature was used to calculate the canopy temperature depression (CTD), the difference between plant canopy temperature and air temperature. Finally, stomatal conductance (g_s) was measured with a Decagon Leaf Porometer SC-1 (Decagon Device Inc., Pullman, WA, USA). One flag leaf was measured for each plot on April 10, April 29, May 23 and May 30, 2013, corresponding to the development stages of jointing, heading, anthesis and post-anthesis, respectively.

2.6. Statistical analysis

All data was analyzed with SPSS 21 (IBM SPSS Statistics 21, Inc., Chicago, IL, USA). Several simple and multiple variance analyses were run to investigate genotypic and the experimental condition

Table 1 – Means and deviations of grain yield (t ha^{-1}) in disease conditions and potential conditions and grain yield loss index (GYLI) of sixteen durum varieties.

Genotype	GY disease conditions	GY potential conditions	GYLI (%)
Iride	6.66 ± 0.58c	6.98 ± 0.61abcd	4 ± 13.29a
Dorondón	6.65 ± 0.51c	6.82 ± 0.58abcd	1.7 ± 13.7a
Pelayo	6.64 ± 0.59c	7.82 ± 0.3de	15 ± 9.54ab
Don Ricardo	6.56 ± 0.81c	7.03 ± 0.56abcd	6.8 ± 5.29a
Simeto	6.48 ± 0.84c	6.72 ± 0.36abc	2.9 ± 18.55a
Kiko Nick	6.48 ± 0.94c	7.61 ± 0.4cde	14.8 ± 9.88ab
Bolo	6.33 ± 0.26c	7.3 ± 0.04abcde	13.2 ± 3.46ab
Regallo	6.33 ± 0.84c	7.51 ± 0.17bcde	15.9 ± 9.62ab
Claudio	6.26 ± 0.37c	7.16 ± 0.63abcde	12.2 ± 6.45ab
Bólido	6.22 ± 0.19c	6.8 ± 0.8abcd	7.6 ± 13.04a
Gallareta	6.14 ± 0.62c	6.84 ± 0.48abcd	10.4 ± 5.89a
Vitrón	5.97 ± 0.16bc	7.09 ± 0.56abcde	15.5 ± 5.55ab
Burgos	5.57 ± 0.68bc	8.08 ± 0.77e	30.3 14.04b
Don Sebastián	5.03 ± 0.13b	6.34 ± 0.8a	19.8 ± 11.8ab
Sula	3.33 ± 0.11a	7.79 ± 0.16de	57.2 ± 1.63c
Don Pedro	2.81 ± 0.1a	6.51 ± 0.33ab	56.8 ± 0.74c
Mean	5.84 ± 1.23	7.15 ± 0.65	17.8 ± 18.5
ANOVA			
Genotype	<0.001	0.009	<0.001

Different letters indicate significant differences within columns according to Duncan's multiple range test ($P < 0.05$).

effects. Duncan post-hoc tests were performed to make multiple correlation comparisons. Pearson correlation coefficient matrices were calculated to look at the multiple bivariate correlations between parameters. Finally, multiple regression analysis with stepwise parameter selection was used in order to develop prediction models for grain yield and grain yield losses.

3. Results

3.1. Grain yield and grain yield loss index

Genotypic differences were found in grain yield in the presence of yellow rust, in potential yield conditions and also in GYLI (Table 1). In the season affected by the yellow rust, there was a difference of 3.85 t ha^{-1} between the most productive genotype and the less productive one. However, in potential conditions, the difference was of 1.74 t ha^{-1} (Table 1). Mean grain losses of all genotypes exceeded 1.3 t ha^{-1}, or on average about 18% of the losses in grain yield. The degree of measured negative effects as measured by GYLI was varied widely between genotypes, ranging between 1.7% (Dorondon) and 57.2% (Sula).

For further description of the parameter relationships a correlation matrix was made between grain yields of in disease-affected season (2012/2013), potential yield conditions (2013/2014 well watered), sub-optimal conditions (2013/2014 rainfed) and GYLI. Grain yield in the disease-affected season did not correlate significantly with potential yield or with sub-optimal yield conditions ($r = 0.065$, $P = 0.662$ and $r = 0.241$, $P = 0.098$, respectively). GYLI was strongly correlated with GY from the disease-affected season ($r = -0.914$; $P < 0.001$) and moderately correlated with potential yield ($r = 0.334$; $P = 0.020$). Potential and sub-optimal yields were marginally correlated ($r = 0.307$; $P = 0.034$).

3.2. Vegetation indices and their relationships with grain yield

The best correlations were clearly found at anthesis (Table 2), whereas the coefficients were lower at the jointing and post-anthesis stages, but GA and GAA were always highly correlated. Significant genotypic differences in GA, GAA and u* were identified at tillering, jointing, anthesis and post-anthesis, whereas significant differences were not detected in hue and a* at the jointing and post-anthesis stages, respectively. We also found genotypic differences in NDVI at tillering and jointing, but not at anthesis.

In general terms, all the measured parameters, especially the RGB indices, fit considerably well to GY and GYLI (Table 3). The parameters that were most strongly correlated to GY and GYLI were GA, GAA and u*, whereas hue, a* and NDVI demonstrated a more variable and less reliable performance. GA proved to be the most reliable RGB index as a predictor of GY and GYLI with the highest coefficients of correlation at all stages. However, the rest of the RGB indices were also very good indicators of GY and GYLI, especially at anthesis, but also at jointing and post-anthesis. NDVI was a good predictor of GY and GYLI at jointing, when disease had not spread, but its effectiveness was considerably lower at anthesis.

Table 2 – P-values from multivariate analysis of variance for genotypes depending on five RGB-based indices, Normalized Difference Vegetation Index (NDVI) as a spectral index and leaf chlorophyll content (LCC), stomatal conductance (g_s) and canopy temperature depression (CTD) as a field measures at five wheat development stages.

	Tillering	Jointing	Heading	Anthesis	Post-anthesis
RGB-indices					
hue	<0.001	0.478	–	<0.001	<0.001
a*	0.004	<0.001	–	<0.001	0.478
u*	0.003	<0.001	–	<0.001	<0.001
GA	<0.001	<0.001	–	<0.001	<0.001
GAA	<0.001	<0.001	–	<0.001	<0.001
Spectral index					
NDVI	0.002	<0.001	–	0.157	–
Field-measures					
LCC	–	0.078	0.002	–	0.116
g_s	–	0.802	0.740	0.616	0.068
CTD	–	–	–	0.885	0.063

Table 3 – Correlations coefficients between RGB-based indices, Normalized Difference Vegetation Index (NDVI), leaf chlorophyll content (LCC), stomatal conductance (g_s), canopy temperature depression (CTD) and grain yield in disease conditions and grain yield loss index (GYLI).

	GY 2012/13 (disease conditions)					GYLI				
	Tillering	Jointing	Heading	Anthesis	Post-anthesis	Tillering	Jointing	Heading	Anthesis	Post-anthesis
RGB-indices										
hue	0.362 *	0.117	–	0.744 **	0.585 **	−0.400 **	−0.069	–	−0.705 **	−0.613 **
a*	−0.345 *	−0.499 **	–	−0.620 **	0.113	0.362 *	0.487 **	–	0.561 **	−0.177
u*	−0.331 *	−0.514 **	–	−0.749 **	−0.601 **	0.356 *	0.507 **	–	0.687 **	0.570 **
GA	0.430 **	0.493 **	–	0.762 **	0.698 **	−0.471 **	−0.521 **	–	−0.732 **	−0.673 **
GAA	0.404 **	0.511 **	–	0.737 **	0.628 **	−0.430 **	−0.523 **	–	−0.681 **	−0.619 **
Spectral index										
NDVI	0.212	0.511 **	–	0.343 *	–	−0.171	−0.526 **	–	−0.357 *	–
Field-measures										
LCC	–	0.079	−0.022	–	0.171	–	−0.001	−0.018	–	−0.200
g_s	–	−0.124	0.095	0.011	0.194	–	0.164	−0.103	−0.109	−0.200
CTD	–	–	–	0.073	0.101	–	–	–	0.001	−0.127

** $P < 0.01$.
* $P < 0.05$.

3.3. *Conventional field-phenotyping parameters and their relationship with grain yield*

Significant genotypic differences in LCC were found only at the heading stage (Table 2). No significant differences g_s were found at any sampling date. Finally, no genotypic differences were found in CTD values at any developmental stage. Despite significant differences in LCC at one growth stage, no significant correlation was found between LCC, g_s, CTD and GY or GYLI at any developmental stage (Table 3).

3.4. *Agronomic parameters and their effect on yield*

Except for the number of spikes per square meter and PH all measured agronomic parameters differed significantly between potential and disease-affected conditions ($P \leq 0.01$) (Table 4). The numbers of grains per square meter, grains per spike, TKW and HI were significantly reduced in disease-affected compared to potent yield conditions. Finally, DH was significantly higher under disease-affected than potential yield conditions.

A Pearson correlation matrix was calculated in order to compare the agronomic parameters with the GY value under biotic-stress (2012/2013 cultivars) and non-biotic-stress conditions (2013/2014 cultivars), and with grain yield losses associated to the presence of rust (Table 5). The GY of disease-affected crops was highly correlated with the number of grains per square meter, spikes per square meter and with HI, moderately correlated with DH and TKW, but not significantly related with number of grains per spike or PH. GYLI showed a strong negative relationship with the number of grains per square meter, spikes per square meter, and with HI, and positively correlated with DH. GYLI showed a trend towards negative relationships with number of grains per spike, TKW and PH, but these are not significant. Regarding potential yield conditions, GY was highly positively related to the number of grains per square meter and moderately correlated with the number of spikes per square meter. However, potential GY was not significantly correlated with the number of grains per spike, TKW, HI, DH or PH.

Finally, the interrelationships between the agronomic parameters themselves in both growing conditions were studied in order to ascribe alteration in these relationships with the presence of disease. Results are shown in Table S1. Relationships between the number of spikes per square meter, grains per spike and HI were maintained in both conditions. DH was negatively related to HI only in disease conditions whereas in potential conditions phenology was only related with PH. For its part, PH was closely correlated in potential conditions with DH, spikes per square meter, grains per spike and with HI; whereas in disease conditions PH was unrelated to the other parameters. Another difference was for TKW which was unrelated to the rest of parameters under disease conditions, but in potential

Table 4 – Mean grains per square meter, grains per spike, spikes per square meter, thousand kernel weight (TKW), harvest index (HI), plant height (PH) and the number of days to heading (DH) under the presence of disease and potential yield conditions. P-values are from multivariate analysis of variance for each agronomic parameter.

	Disease-affected conditions	Potential-yielding conditions	Difference P-value
Grain number (m^{-2})	11,909.40	13,498.90	0.001
Grain number ($spike^{-1}$)	33.35	39.93	<0.001
Spike number (m^{-2})	372.79	348.46	0.204
TKW (g)	44.34	48.07	<0.001
HI (%)	36.04	47.37	<0.001
PH (cm)	101.25	103.23	0.091
DH	154.27	147.10	<0.001

Table 5 – Correlations coefficients between grain yields for potential yielding conditions, disease-affected conditions and grain yield loss index (GYLI) with the number of grains per square meter, grains per spike, spikes per square meter, thousand kernel weight (TKW), harvest index (HI), plant height (PH) and number of days to heading (DH).

	GY disease-affected conditions	GYLI	GY potential-yielding conditions
Spike number (m^{-2})	0.495 **	−0.441 **	0.302 *
Grain number ($spike^{-1}$)	0.203	−0.229	0.082
Grain number (m^{-2})	0.899 **	−0.852 **	0.653 **
TKW	0.298 *	−0.213	0.122
HI	0.513 **	−0.446 **	0.076
DH	−0.345 *	0.333 *	0.086
PH	0.101	−0.156	−0.100

** $P < 0.01$.
* $P < 0.05$.

conditions TKW was highly negatively associated with the number of grains per square meter and the grains per spike.

3.5. Predictive models

With the aim of obtaining a predictive model for grain yield and grain yield losses, we performed a multivariate regression analysis using RGB indices, g_s, NDVI, LCC, CTD, DH and PH as independent variables (Table 6). The best correlated measuring dates with GY and GYLI were chosen for this purpose. For the prediction of GY, the first model selected the RGB-indices GA, GAA, hue and/or u*, always together with DH and was able to explain 69–71% of yield variability in disease conditions ($P < 0.001$). Moreover, the second model explained 60–63% of the variability of grain yield losses by using the RGB-indices GA or hue with DH ($P < 0.001$).

4. Discussion

4.1. Effect of disease on grain yield

The genotypic differences in GY in disease conditions may be largely attributed to the crop sensitivity to yellow rust, as confirmed by the lack of correlations between the GY of the disease-affected field season and the GY of the disease-free field season under both potential and sub-optimal yield conditions. Moreover, as a decrease in PH is usually related to increased water stress [42], the lack of differences in PH between potential and disease conditions suggests that water stress effects under disease conditions were negligible. Potential GY can be considered to scarcely affect the GYLI, since the genotypic variability of potential yield was not related to the observed varietal sensitivity to the disease.

4.2. Performance of vegetation indices

RGB-indices were demonstrated to be the best predictors of grain yield in the presence of yellow rust. The wide range of genotypic differences in most of the RGB-indices at all the growth stages was strongly related with yield variability. NDVI has been used with satisfactory results in many prediction models of yield in wheat at the field level [43], even at regional or state levels [44] using satellite imagery. According to those reports, grain yield could effectively be predicted using NDVI at an early growth stage (jointing), but its accuracy decreased considerably at anthesis (afterwards no data were available). These results were possibly due to a saturation of NDVI in conditions of high biomass [45], as suggested by the narrower confidence interval of NDVI at anthesis (CI = [0.6837, 0.7625]) in comparison to the RGB-index GA (CI = [0.8476, 1.0162]). Moreover, this loss of accuracy may also be attributed to a rapid deterioration of the relationship between NDVI and GY as wheat ripens [46]. In fact, both vegetation index approaches were previously reported to lose accuracy at the late developmental stages [23], but this deterioration in prediction appears to be less pronounced for the RGB indices (from BreedPix software). Therefore, when the ground is totally covered, the information that NDVI provides is more limited, whereas RGB-indices have proved to be even better predictors with dense canopies.

NDVI was previously employed to successfully distinguish between infected, non-infected and N-deficient wheat plots [47]. However, it was mostly used in combined multi-spectral methods with other spectral indices where NDVI acted as a first level biomass sensor in order to discard non-plant spectra [31,32,48] and subsequently the analysis proceeded with the use of other indices. Moreover, these studies based on multi-spectral methods [31,32,48] and previous studies based on digital image analysis [27,29,30] focused on disease detection, leaf classification with regard to infection status and disease level, but its association with yield loss was not described. In this study, the effectiveness of NDVI with regard to GY prediction decreased with disease spread, suggesting

Table 6 – Multivariate regression models explaining grain yield (GY) variation in disease conditions and the grain yield loss index (GYLI) from vegetation indices at anthesis and agronomic traits.

Predicted parameter	Multivariate model	R^2	SEP	F	P-value
GY disease conditions	GY = 27.79 + 0.148 × hue − 0.22 × DH	0.694	0.696	51.13	<0.001
	GY = 26.203 + 3.755 × GAA − 0.179 × DH + 5.113 × GA	0.698	0.700	33.94	<0.001
	GY = 32.021 − 0.291 × u* + 3.355 × GAA − 0.198 × DH	0.709	0.687	35.66	<0.001
GYLI	GYLI = − 302.077 − 2.106 × hue + 3.178 × DH	0.627	11.555	37.78	<0.001
	GYLI = − 173.154 − 154.226 × GA + 2.169 × DH	0.596	12.018	33.22	<0.001

R^2: determination coefficient; SEP: standard error of prediction. RGB-based indices used in these models: GA, GGA, hue and u*. DH: days to heading.

that color changes at the canopy level associated disease spread were missed or omitted by NDVI. Therefore, NDVI may be useful for GY prediction in disease-free conditions and as part of combined methods for disease-detection, but is not an appropriate index of GY assessment in disease-affected conditions. In agreement with previous reports that used digital indices from BreedPix software [23,49] and other image processors [50,51], GY was accurately predicted by RGB indices. As a further contribution, our study demonstrated that RGB indices are also able to predict GY and yield losses in yellow rust infected cultivars at the canopy level. Canopy color characteristics are indicative of the degree of yellow rust infection, thus it was possible to quantify disease severity empirically, and therefore to accurately evaluate grain yield losses in field conditions. Although traditional observational techniques for evaluating crop disease under field conditions have proven to be powerful tools for wheat genotypic selection [52,53], these methodologies are often tedious and difficult to quantify objectively. In this sense, the proposed alternative in this study is particularly interesting for the use in field conditions due to its low cost, precision, rapidity and repeatability.

4.3. *Performance of LCC, g_s and CTD*

LCC is usually related to nitrogen content, photosynthetic capacity and production [54,55]. Previous studies reported a reduction in chlorophyll content in wheat associated with the presence of wheat yellow rust [56]. In our study we note a widespread decrease in LCC of flag leaves at the post-anthesis stage, but this decrease was not correlated with GYLI or GY. Unlike some of the RGB indices, LCC could not describe (according to our methodology) the entire greenness of the plot canopy. In contrast, the water status parameters (g_s and CTD) were insensitive to variation in grain yield. Smith et al. [57] reported the following progression during yellow rust infection: increased transpiration, causing a reduction in temperature due to rupture of the epidermis, followed by overheating of tissues associated with leaf necrosis. On the other hand, recent studies detected leaf temperature changes induced by powdery mildew in wheat under greenhouse conditions by using thermal imaging [58]. Instead, our results suggest that tissue temperature at the canopy level and stomatal conductance were not affected by the amount of disease. Moreover, g_s measurements were time-consuming and surely unrepresentative of the whole plot as only one replicate was measured and weather conditions could oscillate. Thus, these may not be reliable parameters for the selection of varieties resistant to yellow rust under field conditions.

4.4. *Effect of disease on agronomic traits*

Anthesis has widely been reported to be a critical period in determining the number of kernels per spike and the number of kernels per square meter [59], whereas the grain filling period is critical in determining TKW and HI [60]. In our study, disease was detected approximately one month before anthesis, so our results are consistent with previous reports since grain yield losses were mainly associated with reductions in the number of grains per spike, TKW, HI and grains per square meter (Table 4). Contrary to previous reports [61] wherein infection began at a very early growth stage, the number of spikes per square meter was not significantly decreased in our study. The favorable growing conditions during tillering and before disease spread enabled good establishment of tillers, which could explain the high number of spikes per square meter [62–64] as it is comparable to potential yielding conditions. In summary, our results suggest that the reduction in grain yield in disease conditions was probably due to: (i) increased grain abortion (or reduction in fertility) shown by a reduction of grains per spike and grains per square meter and (ii) a reduction in the amount of photoassimilates [65] intended for grain filling, explaining the reductions in TKW and HI.

The contribution of each agronomic parameter to variation in grain yield showed clear differences depending on the experimental conditions (Table 5). The main difference lies in the correlation of DH, TKW and HI with GY, which occurred only in the disease presence. Moreover, in the disease-affected trial we noted a significant negative relationship between HI and DH (Table S1), which suggested that early heading enabled a degree of disease escape, and made it possible for the plants to achieve a greater HI and thereby achieve higher yields in these conditions. This highlights the importance of wheat phenology for avoiding stress conditions [57], whereas in good agronomic conditions, the phenological characteristics were not good determinants of yield. In contrast, the rest of the agronomic parameters showed similar trends in relation to grain yield in all conditions. The yield component compensation principle [66] explains that the strong cross-correlation between spikes per square meter, grains per spike and HI remained robust even in the presence of disease.

4.5. *Predictive model assessment*

Finally, the multivariate regression models revealed the most appropriate parameters for field phenotyping in the presence of yellow rust. Yield was ignored in this model because the main interest was to assess GY and GYLI using independent traits measured before maturity. The development of yellow rust involves gradual changes in the color characteristics of crop canopies as epidemics' progress, and this information is obtained by the RGB-indices. According to the results of multivariate models, information contained in the RGB-indices, together with phenology, are closely related to GY and GYLI as the predictions are robust (R^2 = 0.6 and R^2 =0.7; respectively) and reliable ($P < 0.001$). Both models demonstrated the potential of digital vegetation indices to characterize biotic stress produced by yellow rust, its utility for grain yield losses assessment and, therefore, selection of resistant varieties. Although the correlations of DH with GY and GYLI were mild, all regression models chose DH as a predictive parameter; so, our study suggests that this phenological trait provides a: (i) different information compared to the rest of the included parameters, (ii) useful data and (iii) information related to grain yield in biotic stress conditions.

5. Conclusions

The Warrior/Ambition strain of *P. striiformis* f. sp. *tritici* seriously affected most of the genotypes of our collection. For some

genotypes it resulted in losses greater than 50% of the potential yield. This highlights the need to find genotypically resistant varieties by using high throughput phenotyping tools such as those used in the present study. For the first time, RGB-indices demonstrated the potential of using digital images of crop canopies instead of pictures and scans of isolated leaves or conventional observational evaluations for GY assessment in infected disease nurseries. This represents a marked advantage as this procedure has also been shown to be: (i) considerably faster, (ii) more representative of the whole plot, and (iii) more objective than those mentioned above. Unlike NDVI, which is much less efficient by itself, digital indices provide accurate and useful information for wheat breeding with dense canopy coverage. Moreover, LCC, g_s and CTD proved to be inappropriate for grain yield loss assessments in the presence of yellow rust. We also demonstrated the association of the presence of the wheat yellow rust disease to changes in the interrelationships between agronomic traits themselves and their contribution to grain yield compared to potential conditions. To the best of our knowledge this is the first report showing that phenology can play a significant role with regard to biotic stress conditions in wheat. Finally, the optimal yield predictive models include DH always together with RGB indices and they set robust and reliable predictions. The versatility, low cost, and high throughput of digital RGB techniques show promise as potentially useful tools in many agronomic areas, and should be considered in future phenotyping strategies.

Acknowledgments

This study was supported by the Spanish project AGL2013-44147-R. We thank Jesús Vega, head of INIA Station at Aranjuez, José Novo and our partners, Dr. Salima Yousfi, Rut Sánchez-Bragado, Dr. Jordi Bort and Bangwei Zhou, for their assistance with the collection of phenotic data during the study. We also thank Dr. Isabel Trillas and Dr. Néstor Hladun for their help in fungus verification. Finally we thank Dr. Jaume Casadesús for providing the BreedPix software.

Supplementary material

Supplementary material to this article can be found online at http://dx.doi.org/10.1016/j.cj.2015.03.003.

REFERENCES

[1] Survey about surfaces and crop yields in Spain (ESYRCE), Framework Survey of Areas in Spain, Publication prepared by the Technical Secretariat, General Statistics Branch, Madrid 2013Ministry of Agriculture, Food and Environment, Government of Spain, 2013.
[2] FAO, Statistical yearbook 2013, World Food and Agriculture, FAO, Rome, 2013.
[3] J. Almacellas, A. López, F. Álvaro, J. Serra, G. Capellades, J. Marín, Yellow rust of wheat, an emerging problem (La roya amarilla de los trigos, un problema emergente; Vida Rural), Rural Life publication, by Agronline, Winter wheat Dossier, num., 370, November 2013.
[4] J.G. Hansen, P. Lassen, M. Hovmoller, D. Hodson, ICT framework for global wheat rust surveillance and monitoring, 10th Conference of European Foundation for Plant Pathology, Wageningen, The Netherlands, 2012.
[5] E. Sanchez-Monge, Evolution of wheat yellow rust virulence in Spain: 2010–2013 (Evolución de la virulencia a la roya amarilla del Trigo en España: 2010–2013), Limagrain, Ibérica, 2013.
[6] M.S. Hovmøller, A.F. Justesen, J.K.M. Brown, Clonality and long-distance migration of *Puccinia striiformis* f. sp. *tritici* in north-west Europe, Plant Pathol. 51 (2002) 24–32.
[7] W. Chen, C. Wellings, X. Chen, Z. Kang, T. Liu, Wheat stripe (yellow) rust caused by *Puccinia striiformis* f. sp. *tritici*, Mol. Plant Pathol. 15 (2014) 433–446.
[8] N. Aparicio Gutierrez, C. Carnicero Saldaña, F.J. Puertas Jorde, Yellow rust development on the wheats of Castilla y León (El desarrollo de la roya amarilla en los trigos de Castilla y León), Agricultural Technology Institute (ITA), Government of Castilla y León, Ministry of Agriculture and Livestock, Valladolid, May 2014.
[9] J.L. Araus, J. Cairns, Field high-throughput phenotyping—the new crop breeding frontier, Trends Plant Sci. 19 (2014) 52–61.
[10] J.L. Araus, G.A. Slafer, C. Royo, M.D. Serret, Breeding for yield potential and stress adaptation in cereals, Crit. Rev. Plant Sci. 27 (2008) 1–36.
[11] L. Cabrera-Bosquet, J. Crossa, J. von Zitzewitz, M.D. Serret, J.L. Araus, High-throughput phenotyping and genomic selection: the frontiers of crop breeding converge, J. Integr. Plant Biol. 54 (2012) 312–320.
[12] J.N. Cobb, G. DeClerck, A. Greenberg, R. Clark, S. McCouch, Next-generation phenotyping: requirements and strategies for enhancing our understanding of genotype–phenotype relationships and its relevance to crop improvement, Theor. Appl. Genet. 126 (2013) 867–887.
[13] R.T. Furbank, M. Tester, Phenomics — technologies to relieve the phenotyping bottleneck, Trends Plant Sci. 16 (2011) 635–644.
[14] G.A. Carter, Reflectance wavebands and indices for remote estimation of photosynthesis and stomatal conductance in pine canopies, Remote Sens. Environ. 63 (1998) 61–72.
[15] A.R. Huete, A soil adjusted vegetation index (SAVI), Remote Sens. Environ. 25 (1988) 295–309.
[16] J.A. Gamon, J. Peñuelas, C.B. Field, A narrow waveband spectral index that tracks diurnal changes in photosynthetic efficiency, Remote Sens. Environ. 41 (1992) 35–44.
[17] W. Huang, D.W. Lamb, N. Zheng, Y. Zhang, L. Liu, J. Wang, Identification of yellow rust in wheat using in-situ spectral reflectance measurements and airborne hyperspectral imaging, Precis. Agric. 8 (2007) 187–197.
[18] J. Peñuelas, J.A. Gamon, K.L. Griffin, C.B. Field, Assessing type, biomass, pigment composition and photosynthetic efficiency of aquatic vegetation from spectral reflectance, Remote Sens. Environ. 46 (1993) 110–118.
[19] J. Peñuelas, I. Filella, J.A. Gamon, Assessment of photosynthetic radiation — use efficiency with spectral reflectance, New Phytol. 131 (1995) 291–296.
[20] E.W. Chappelle, M.S. Kim, J.E. McMurtrey III, Ratio analysis of reflectance spectra (RARS): an algorithm for the remote estimation of the concentrations of chlorophyll A, chlorophyll B, and carotenoids in soybean leaves, Remote Sens. Environ. 39 (1992) 239–247.
[21] J. Casadesús, C. Biel, R. Savé, Turf color measurement with conventional digital cameras, in: J. Boaventura (Ed.), EFITA/WCCA Joint Congress on IT in Agriculture, Vila Real, Portugal, 2005.
[22] USDA, Foreign Agricultural Service, Ethiopia 2008 Crop Assessment Travel Report, 2008.

[23] J. Casadesus, Y. Kaya, J. Bort, M.M. Nachit, J.L. Araus, S. Amor, G. Ferrazzano, F. Maalouf, M. Maccaferri, V. Martos, H. Ouabbou, D. Villegas, Using vegetation indices derived from conventional digital cameras as selection criteria for wheat breeding in water-limited environments, Ann. Appl. Biol. 150 (2007) 227–236.
[24] F.J. Adamsen, P.J. Pinter, E.M. Barnes, R.L. LaMorte, G.W. Wall, S.W. Leavitt, B.A. Kimball, Measuring wheat senescence with a digital camera, Crop Sci. 39 (1999) 719–724.
[25] Managing Lodging Risk in Winter Wheat, Featuring the new Canopy Assessment Tool, Developed by BASF plc Crop Protection in collaboration with ADAS, http://www.pgrplus.basf.com/.
[26] M. Gils, K. Kempe, A. Boudichevskaia, R. Jerchel, D. Pescianschi, R. Schmidt, M. Kirchhoff, R. Schachschneider, Quantitative assessment of wheat pollen shed by digital image analysis of trapped airborne pollen grains, Adv. Crop Sci. Tech. 2, (2013)http://dx.doi.org/10.4172/2329-8863.1000119.
[27] H. Kampmann, O.B. Hansen, Using colour image analysis for quantitative assessment of powdery mildew on cucumber, Euphytica 79 (1994) 19–27.
[28] P. Vincelli, D.E. Hershman, Assessing Foliar Diseases of Corn, Soybeans and Wheat, Plant Pathology Fact Sheet, University of Kentucky, College of Agriculture, November 2011.
[29] V. Maloney, S. Petersen, R.A. Navarro, D. Marshall, A.L. McKendry, J.M. Costa, J.P. Murphy, Digital image analysis method for estimation of Fusarium-damaged kernels in wheat, Crop Sci. 54 (2014) 2077–2083.
[30] E.L. Stewart, B.A. McDonald, Measuring quantitative virulence in the wheat pathogen *Zymoseptoria tritici* using high-throughput automated image analysis, Phytopathology 104 (2014) 985–992.
[31] D.M. Ashourloo, R. Mobasheri, A. Huete, Evaluating the effect of different wheat rust disease symptoms on vegetation indices using hyperspectral measurements, Remote Sens. Environ. 6 (2014) 5107–5123.
[32] D. Moshou, C. Bravo, R. Oberti, J. West, L. Bodria, A. McCartney, H. Ramon, Plant disease detection based on data fusion of hyper-spectral and multi-spectral fluorescence imaging using Kohonen maps, Real-Time Imaging 11 (2005) 75–83.
[33] T. Mahmood, D. Marshall, Remote assessment of leaf rust of wheat in cultivars mixture and component purelines, Pak. J. Agric. Sci. 40 (2003) 63–66.
[34] M. Mirik, G.J. Michels, S. Kassymzhanova-Mirik, D. Jones, N.C. Elliott, V. Catana, R. Bowling, Hyperspectral field spectrometry for estimating greenbug (Homompeta: Aphidae) damage in wheat. in: 20th Biennial Workshop on Aerial Photography, Videography, and High Resolution Digital Imagery for Resource Assessment October 4–6, 2005, Weslaco, Texas.
[35] C.H. Bock, G.H. Poole, P.E. Parker, T.R. Gottwald, Plant disease severity estimated visually, by digital photography and image analysis, and by hyperspectral imaging, Crit. Rev. Plant Sci. 29 (2010) 59–107.
[36] C. Trueba, R. Millán, T. Schmid, C. Roquero, M. Magister, Database of Pedology Properties of Spanish soils (Base de Datos de Propiedades Edafológicas de los Suelos Españoles), Volume V. Madrid, Department of Environmental Impact of Energy, December, 1998.
[37] United States Department of Agriculture, Natural Resources Conservation Service, Keys to Soil Taxonomy, 10th edition, 2006.
[38] Agro-climatic Information System for Irrigation (Sistema de Información Agroclimática para el Regadío, SIAR) (http://eportal.magrama.gob.es/websiar/). Ministry of Agriculture, Food and Environment, Government of Spain and the European Agricultural Fund for Rural Development (Last consulted on August 2014).
[39] Group for the Evaluation of New Varieties of Extensive Crops in Spain (Grupo para la Evaluación de Nuevas Variedades de Cultivos Extensivos en España — GENVCE), http://www.genvce.org/.
[40] L. O'Gorman, M.J. Sammon, M. Seul, Practical Algorithms for Image Analysis: Description, Examples and Code, Second edition Cambridge University Press, Cambridge, 2000.
[41] M.J. Vrhel, E. Saber, H.J. Trussell, Color image generation and display technologies, IEEE Signal Process. Mag. (January 2005) 23–33.
[42] N.K. Gupta, S. Gupta, A. Kumar, Effect of water stress on physiological attributes and their relationship with growth and yield of wheat cultivars at different stages, J. Agron. Crop Sci. 186 (2001) 55–62.
[43] N. Aparicio, D. Villegas, J. Casadesus, J.L. Araus, C. Royo, Spectral vegetation indices as nondestructive tools for determining durum wheat yield, Agron. J. 92 (2000) 83–91.
[44] M. Moriondo, F. Maselli, M. Bindi, A simple model of regional wheat yield based on NDVI data, Eur. J. Agron. 26 (2007) 266–274.
[45] T. Hobbs, The use of NOAA-AVHRR NDVI data to assess herbage production in the arid rangelands of Central Australia, Int. J. Remote Sens. 16 (1995) 1289–1302.
[46] J.K. Aase, F.H. Siddoway, Assessing winter wheat dry matter production via spectral reflectance measurements, Remote Sens. Environ. 11 (1981) 267–277.
[47] J. Jacobi, W. Kühbauch, Site-specific identification of fungal infection and nitrogen deficiency in wheat crop using remote sensing, in: J.V. Stafford (Ed.), Proceedings of the 5th European Conference on Precision Agriculture, Wageningen Academic Publishers, The Netherlands 2005, pp. 73–80.
[48] J. Franke, G. Menz, Multi-temporal wheat disease detection by multi-spectral remote sensing, Precis. Agric. 8 (2007) 161–172.
[49] A. Morgounov, N. Gummadov, S. Belen, Y. Kaya, M. Keser, J. Mursalova, Association of digital photo parameters and NDVI with winter wheat grain yield in variable environments, Turk. J. Agric. For. 38 (2014) 624–632.
[50] T. Jensen, A. Apan, F. Young, L. Zeller, Detecting the attributes of a wheat crop using digital imagery acquired from a low-altitude platform, Comput. Electron. Agric. 59 (2007) 66–77.
[51] G. Pan, F.M. Li, G.J. Sun, Digital camera based measurement of crop cover for wheat yield prediction, Geoscience and Remote Sensing Symposium, 2007. IGARSS 2007IEEE International 23–28 July 2007, pp. 797–800, http://dx.doi.org/10.1109/IGARSS.2007.4422917.
[52] S. Ali, S.J.A. Shah, K. Maqbool, Field-based assessment of partial resistance to yellow rust in wheat germplasm, J. Agric. Rural. Dev. 6 (2008) 99–106.
[53] F.M. Nzuve, S. Bhavani, G. Tusiime, P. Njau, Field screening of bread wheat for partial sources of resistance to stem rust, Research Application Summary, Third Ruforum Biennal Meeting, 24–28 September 2012, Entebbe, Uganda.
[54] J.R. Evans, Nitrogen and photosynthesis in the flag leaf of wheat, Plant Physiol. 72 (1983) 297–302.
[55] J.R. Seemann, T.D. Sharkey, J. Wang, C.B. Osmond, Environmental effects on photosynthesis, nitrogen-use efficiency, and metabolite pools in leaves of sun and shade plants, Plant Physiol. 84 (1987) 796–802.
[56] M.T. McGrath, S.P. Pennypacker, Alteration of physiological processes in wheat flag leaves caused by stem rust and leaf rust, Phytopathology 80 (1989) 677–686.
[57] R.C.G. Smith, A.D. Heritage, M. Stapper, H.D. Barrs, Effect of stripe rust (*Puccinia striiformis* West.) and irrigation on the yield and foliage temperature of wheat, Field Crop Res. 14 (1986) 39–51.

[58] Y.M. Awad, A.A. Abdullah, T.Y. Bayoumi, K. Abd-Elsalam, A.E. Hassanien, Early detection of powdery mildew disease in wheat (*Triticum aestivum* L.) using thermal imaging techniques, Intelligent Systems' 2014, Advances in Intelligent Systems and ComputingSpringer International Publishing, Cham, Switzerland 2015, pp. 755–765.
[59] S.A. Herrera-Foessel, R.P. Singh, J. Huerta-Espino, J. Crossa, J. Yuen, A. Djurle, Effect of leaf rust on grain yield and yield traits of durum wheats with race-specific and slow-rusting resistance to leaf rust, Plant Dis. 90 (2006) 1065–1072.
[60] R.A. Fischer, Selection traits for improving yield potential, in: M.P. Reynolds, J.I. Ortiz-Monasterio, A. McNab (Eds.), Application of Physiology in Wheat Breeding, CIMMYT, Mexico, 2001.
[61] R.P. Singh, J. Huerta-Espino, Effect of leaf rust gene *Lr34* on grain yield and agronomic traits of spring wheat, Crop Sci. 37 (1994) 390–395.
[62] S. Elhani, V. Martos, Y. Rharrabti, C. Royo, L.F. García del Moral, Contribution of main stem and tillers to durum wheat (*Triticum turgidum* L. var. *Durum*) grain yield and its components grown in Mediterranean environments, Field Crop Res. 103 (2007) 25–35.
[63] R.A. Richards, A.G. Condon, G.J. Rebetzke, Traits to improve yield in dry environments, in: M.P. Reynolds, J.I. Ortiz-Monasterio, A. McNab (Eds.), Application of Physiology in Wheat Breeding, CIMMYT, Mexico 2001, pp. 88–100.
[64] B.L. Duggan, R.A. Richards, A.F. van Herwaarden, N.A. Fettell, Agronomic evaluation of a tiller inhibition gene (Tin) in wheat: I. Effect on yield, yield components, and grain protein, Aust. J. Agric. Res. 56 (2005) 169–178.
[65] R.E. Gaunt, The relationship between plant disease severity and yield, Annu. Rev. Phytopathol. 33 (1995) 119–144.
[66] M.W. Adams, Basis of yield component compensation in crop plants with special reference to field bean, *Phaseolus vulgaris*, Crop Sci. 7 (1967) 505–510.